Inverse scattering for a specific resonating group model nonlocality

G. Pantis* and S. A. Sofianos
Department of Physics, University of South Africa, Pretoria, South Africa
(Received 6 March 1996)

An inverse scattering method of Lipperheide and Fiedeldey [Z. Phys. A **286**, 45 (1978); **301**, 81 (1981)] has been used to construct an energy-dependent potential from the elastic-scattering phase shifts of the recently developed K model of Kaneko, LeMere, and Tang [Phys. Rev. C **44**, 1588 (1991); **46**, 298 (1992)] for the $n-\alpha$ and $n-{}^{40}$Ca systems. The local momentum of the inversion potential is subsequently used to recover the Wigner transforms of the K model. The results obtained indicate that it is possible to find, via inversion, an l-independent Wigner transform, which, when calculated at all energies, can provide us with the full nonlocality. [S0556-2813(96)02010-9]

PACS number(s): 24.10.−i, 03.80.+r, 21.30.Fe, 25.40.Dn

I. INTRODUCTION

There are nowadays many applications of the inverse-scattering problem with potential scattering theory, i.e., the determination of a potential from its phase shifts, in the literature. Although some of them refer to nonlocal potentials of diverse type [1], the majority deal with local potentials. In nuclear scattering, however, the underlying interaction in general is nonlocal the form of which depends upon the nature of the problem. For example, in nucleon-nucleus and nucleus-nucleus reactions the optical model potentials are nonlocal, when they are derived microscopically, but there are diverse approaches to specify those nonlocal interactions [2]. Whatever their form, however, those nonlocal interactions usually have a quite complicated structure. That makes them cumbersome to use and thus one resorts either to construction of local equivalent potentials or to other simplifications, a typical example of which is the K model of Kaneko *et al.* [3]. That is a simplified version of the resonating group model (RGM), but it has analytic properties that enable it to be used in a straightforward way to study several aspects of nucleon-nucleus scattering [4,5].

An initial attempt to apply inverse-scattering techniques to retrieve information on the underlying nonlocality of the scattering potential was made by Fiedeldey *et al.* [1]. In that work the $n-\alpha$ nonlocal interaction of Lassaut and Vinh Mau [6] was employed to obtain the phase shifts, which then were used to construct a local potential $V_L(E,r)$ by inversion, the energy dependence of which reflected the associated nonlocality. This procedure can be used only when the nonlocality is independent of energy. Fiedeldey *et al.* [1] had shown that a nonlocal energy-independent potential of the Frahn-Lemmer type can be determined from its phase shifts if these are given at all angular momenta and at all energies. This method represents a solution of the inverse-scattering problem for a specified class of nonlocal interactions within the WKB approximation. But if the nonlocality intrinsically is energy dependent, the phase shifts do not contain enough information for the implementation of the scheme. In the present work we investigate whether or not a similar inversion procedure can reproduce the nonlocality of the K model from its phase shifts $\delta_l(k)$. For this purpose we use the phase shifts to generate by inversion a local energy-dependent potential $V_I(E,R)$ and from its local momentum $p(E,R)$ we obtain the Wigner transform $V^W[R^2,p^2(E,R)]$. For comparison purposes we also construct the equivalent local potential $V_L(E,R)$ obtained via the Horiuchi WKB approximation [7]. The subscripts I and L designate ''inversion'' and ''local,'' respectively. The inversion scheme has been applied in two cases, namely, the scattering of neutrons from α particles and ^{40}Ca nuclei for which analytical expressions for the K model are available. We note that the $n-\alpha$ system with a nonlocality derived in the antisymmetrized folding model was treated along the same lines in Ref. [1].

We mention here that several works on nucleon-nucleus scattering have appeared recently utilizing complex nonlocal potentials. In particular we refer to the works of Karataglidis *et al.* [8], which gave excellent fits to elastic and inelastic proton scattering on ^{12}C, ^{14}N, and ^{16}O. In these analyses both the elastic-scattering optical model potentials and the inelastic scattering amplitudes were evaluated fully microscopically using an effective nucleon-nucleon (NN) interaction developed from the mapping of the NN g matrices of the Paris potential for diverse infinite nuclear matter densities. The optical potentials resulting from folding the effective interaction with the target density were nonlocal and the associated nonlocal Schrödinger equation was solved. Nevertheless, although the reported results are excellent, there is much more effort involved in these calculations than, for example, in the K-model applications of Ref. [5].

The situation becomes even more involved for higher target nuclei or for nucleus-nucleus reactions. Examples for this are the semimicroscopic works of Pantis and Pearson [9] for the ^{12}C-^{12}C, ^{16}O-^{16}O, and ^{12}C-^{16}O reactions in which the interactions were based upon a fit to the NN scattering amplitudes by a sum of Yukawa potentials and of Bohlem *et al.* [10] for the ^{16}O-^{16}O and ^{12}C-^{20}Ne reactions where an oversimplistic picture of the underlying g matrices for folded potentials is used. The same is true for the fully microscopic calculation in the nuclear matter approach of Ref. [11] for the ^{12}C-^{12}C reaction that required the inclusion of polarization potentials arising from the excitation of the 3α breakup

*Permanent address: Department of Physics, University of Ioannina, 45110, Ioannina, Greece.

states to improve the agreement with the experimental data.

In the present work it will be shown that the nonlocal interactions obtained for both scattering systems yield equivalent local potentials, in good agreement with the inversion results, at least for the energies at which the inversion has been carried out. In fact, for the $n-{}^{40}$Ca system the equivalent local potentials are almost identical. Our work therefore complements and generalizes that of Ref. [1], in which the inversion scheme was applied to a nonlocal potential of the Frahn-Lemmer type. In Sec. II we briefly outline our formalism and present the localization procedures, the Wigner transform of the K model, and the inversion method used.

In Sec. III we present our results and the discussions of them. Finally, in Sec. IV we summarize our conclusions.

II. FORMALISM

Resonating group method calculations [1] lead to optical potentials for nuclear scattering that are nonlocal with the nonlocality being energy dependent in general and the Wigner transform of the type $V^W[R^2,p^2,(\mathbf{p}\cdot\mathbf{R})^2]$ being l dependent. Global inverse scattering theories, when applied with the scattering phase shifts found from such potentials however, yield energy-dependent local interactions from which an l-independent Wigner transform results. The RGM of Kaneko *et al.* [3,4], designated as the K model hereinafter, is a special case for which the nonlocality is independent of energy. Furthermore, the Wigner transform is independent of l. With the K model, therefore, a direct comparison of the two nonlocalities, namely, the original K model and the one obtained by inversion, is possible.

Using the stationary Hamilton-Jacobi equation [7], in the semiclassical approximation in zeroth order of $\hbar$, the Wigner transform enters the energy equation by

$$\frac{p^2}{2\mu}+V^W(R^2,p^2)=E. \tag{1}$$

This relation gives the local momentum $p(E,R)$ as a function of the radius R at a given energy E. A semiclassical equivalent local potential $V_L(E,R)$ can be found iteratively using the Wigner transform of the original nonlocal interaction

$$V_L(E,R)=V^W(R^2,p^2), \tag{2}$$

with

$$\frac{p^2}{2\mu}=[E-V_L(E,R)]. \tag{3}$$

Then if the inversion potential $V_I(E,R)$ produces equivalent localized function $p^2(E,R)$ as does use of the potential $V_L(E,R)$,

$$V_I(E,R)=V^W(R^2,2\mu[E-V_I(E,R)]). \tag{4}$$

Thus a numerical evaluation of the Wigner transform from Eq. (4) for a sufficiently large number of energies can provide, via Fourier transformation, the nonlocality of the original potential. In this work we do not carry out the full program. We will instead demonstrate its feasibility for two different systems with different characteristics and at two different energies. For completeness, in Secs. II A and II B, brief reviews are given of the Wigner transforms for the K model and of the inversion scheme used.

A. The K model

In the K-model approximation to the RGM nonlocality, recoil effects are neglected and only direct and knock-on exchange effects are taken into account. Using a local nucleon-nucleon potential of the form

$$V_{ij}=-V_0\exp(-\kappa r_{ij}^2)(w-mP_{ij}^{\sigma}P_{ij}^{\tau}+bP_{ij}^{\sigma}-hP_{ij}^{\tau}) -\frac{1}{2\hbar}V_{\lambda}\exp(-\lambda r_{ij}^2)(\sigma_i+\sigma_j)\cdot(\mathbf{r}_i-\mathbf{r}_j)\times(\mathbf{p}_i-\mathbf{p}_j), \tag{5}$$

wherein κ and λ are inverse square ranges and P_{ij}^x are the usual spin and isospin projection operators, the resulting K-model nonlocal interaction consists of three terms: the direct term $V_D(R)$, the exchange term $V_{\rm ex}(\mathbf{r},\mathbf{r}')$, and the spin-orbit term $V_{\rm SO}(R)$. The expressions for the nonlocal kernels for the systems under consideration are given in Ref. [3]. Here we note that their Wigner transforms are defined by

$$V^W[\mathbf{R},\mathbf{p}(\mathbf{R})]\equiv\int d\mathbf{s}\exp(i\mathbf{s}\cdot\mathbf{p}/\hbar)V_{\rm ex}\left(\mathbf{R}-\frac{1}{2}\mathbf{s},\mathbf{R}+\frac{1}{2}\mathbf{s}\right) \tag{6}$$

and are derived as outlined in the Appendix of Ref. [12]. In our applications, Eq. (6) has been used with the exchange potentials obtained from the K model and for which the Wigner transform takes the form $V^W(R^2,p^2)$. For the two cases of interest, the results are given next.

For the $n-\alpha$ system, the various terms resulting from use of the K model are

$$V_D(R)=-V_0\gamma(4w-m-2b-2h)\exp\left(-\frac{\alpha\kappa}{\alpha+\kappa}R^2\right), \tag{7}$$

$$V^W(R^2,q^2)=-V_0\beta(-w+4m-2b+2h)\times\exp\left(-\alpha R^2-\frac{q^2}{B}\right), \tag{8}$$

and

$$V_{\rm SO}(R)=-2J_{\lambda}\alpha^{5/2}\exp(-\alpha R^2), \tag{9}$$

where $q^2=p^2/\hbar^2$. For the $n-{}^{40}$Ca scattering, the K model yields [5]

$$V_D(R)=-V_0\gamma(4w-m+2b-2h)\left[\frac{5}{2}+\frac{15\alpha^2}{2(\alpha+\kappa)^2}+\frac{10\alpha^2\kappa^2}{(\alpha+\kappa)^3}R^2+\frac{2\alpha^2\kappa^4}{(\alpha+\kappa)^4}R^4\right]\exp\left(-\frac{\alpha\kappa}{\alpha+\kappa}R^2\right), \tag{10}$$

$$V^W(R^2,q^2)=-V_0\beta(-w+4m-2b+2h)\times\exp\left(-\alpha R^2-\frac{q^2}{4B}\right)\times\left\{\frac{5}{2}+\alpha\left(-\frac{3}{2B}+\frac{q^2}{(2B)^2}\right)+2\alpha^2\left[\left(-\frac{3}{8B}+R^2+\frac{q^2}{(4B)^2}\right)^2-\left(\frac{-3}{2(4B)^2}+\frac{q^2}{4(2B)^3}\right)\right]\right\},$$

and

$$V_{\rm SO}(R)=-2J_\lambda\alpha^{5/2}(2\alpha^2R^4-4\alpha R^2-5/2)\exp(-\alpha R^2). \tag{11}$$

The parameter α is the RGM oscillator parameter, $\gamma=[\alpha/(\alpha+\kappa)]^{3/2}$, $\beta=(\alpha/B)^{3/2}$, and $B=\alpha+4\kappa$. The parameter $J_\lambda=V_\lambda\lambda^{3/2}$ is derived on the basis of the zero-range approximation for the spin-orbit force and is determined phenomenologically. Note that as the Wigner transforms for both systems do not depend on the product $\mathbf{q}\cdot\mathbf{R}$, the corresponding equivalent local potentials will be l independent.

B. The inversion scheme

To construct the inversion potential $V_I(E,R)$ from the phase shifts we employ the fixed-energy inversion scheme of Lipperheide and Fiedeldey [13]. In this scheme the Schrödinger equation for a complex angular momentum λ is written as

$$\left[\frac{d^2}{dr^2}-\frac{\lambda^2-\frac{1}{4}}{r^2}-U(r)\right]u(\lambda,k;r)=0\,, \tag{12}$$

where $U(r)=2\mu/\hbar^2V(r)$, $V(r)$ is the potential, and μ is the effective mass. The associated scattering function or S function is given by

$$S(\lambda,k)=\frac{\mathcal{F}(\lambda,-k)}{\mathcal{F}(\lambda,+k)}, \tag{13}$$

where the Jost function $\mathcal{F}$ is related to the Jost solutions

$$f(\lambda,\pm k,r)\underset{r\to\infty}{\to}\exp(\pm ikr) \tag{14}$$

via

$$\mathcal{F}(\lambda,k)=-2\lambda\lim_{r\to0}r^{\lambda-1/2}f(\lambda,k;r) \tag{15}$$

for $\mathrm{Re}\lambda>0$. To proceed in the Lipperheide-Fiedeldey inversion, one chooses a particular parametrized form for the S function such as the rational parametrization, which is similar to the Bargmann class of solvable potentials at fixed angular momentum. A convenient representation is

$$S^{\rm rat}(\lambda)=S^{(0)}(\lambda)\prod_{n=1}^{N}\frac{\lambda^2-\beta_n^2}{\lambda^2-\alpha_n^2}, \tag{16}$$

where $S^{(0)}(\lambda)$ represents a background S function corresponding to a potential $V_0(r)$ (e.g., the Coulomb potential for a charged sphere). Other, more general, parametrizations are the ''nonrational'' and the ''mixed rational and nonrational'' schemes [14]. This rational form of S function relates to a potential

$$V(E,r)=V_N(E,r), \tag{17}$$

where $V_N(E,r)$ is obtained by the recursion formula

$$V_n(E,r)=V_{n-1}(E,r)+V^{(n)}(E,r),\quad n=1,2,\ldots,N, \tag{18}$$

which involves the residue

$$V^{(n)}(E,r)=\frac{2i}{r}(\beta_n^2-\alpha_n^2)\frac{d}{dr}\left[\frac{1}{r}\frac{1}{L_{\beta_n}^{(-)(n-1)}+L_{\alpha_n}^{(+)(n-1)}}\right]. \tag{19}$$

The functions $L_\lambda^{(\pm)(n)}(r)$ are logarithmic derivatives of the Jost functions behaving as $e^{\mp ikr}$ as $r\to\infty$. They satisfy a Riccati equation

$$\mp\frac{d}{dr}L_\lambda^{(\pm)(n)}-[L_\lambda^{(\pm)(n)}]^2+1-V_n(r)-\frac{\lambda^2-\frac{1}{4}}{r^2}=0\,. \tag{20}$$

The task then is to find a set of complex pole and zero pairs from the scattering data. One finds those by using the phase shifts $\delta_l(k)$ or equivalently, the S function, as described in the Appendix.

III. RESULTS

The K model was used to specify nonlocal $n-\alpha$ and $n-{}^{40}$Ca potentials and the nucleon-nucleon potential parameters used were $w=m=0.4075$, $b=h=0.0925$, and $\kappa=0.46$ fm^{-2}, while the depth of the potential was taken to be $V_0=72.98$ MeV. For the $n-\alpha$ system the RGM oscillator parameter α was fixed at $\alpha=0.685$ fm^{-2} and the spin-orbit parameter J_λ was set to zero. For the $n-{}^{40}$Ca system, we used $\alpha=0.253$ fm^{-2} and $J_\lambda=50$ MeV fm^5. The parameters employed in Ref. [5] were readjusted to take into account dispersive corrections to the optical potential. There the oscillator parameter giving the best fit to the cross sections was found to be $\alpha=0.231$ fm^{-2}. The resulting optical potential [5] has an energy-dependent depth stemming from the volume and surface dispersive corrections. It will be seen that the equivalent local potential obtained in this work has almost the same depth.

The phase shifts that result by using the K-model potentials, the S-function fits, and from the inversion studies are given in Tables I–IV. It is seen that the reproductions of the input (K-model) phase shifts δ_K by the S-function parametri-

TABLE I. $n-\alpha$ phase shifts, in degrees, at incident neutron energy $E_n=50$ MeV. The δ_K are the input phase shifts of the K model; the $\delta_{\rm fit}$ is the reproduction by the parametrization of the S function, while δ_I is the reproduction by the inversion potential $V_I(E,R)$.

l	δ_K	$\delta_{\rm fit}$	$\delta_K-\delta_{\rm fit}$	δ_I	$\delta_K-\delta_I$
0	73.987	76.231	2.244	70.873	-3.114
1	58.846	58.138	-0.708	57.922	-0.924
2	27 179	26.232	-0.947	28.018	-0.839
3	8.237	8.102	-0.135	8.587	0.350
3	2.133	2.379	0.247	2.182	0.049
4	0.490	0.635	0.165	0.495	0.005
5	0.100	0.168	0.068	0.100	0.000
6	0.018	0.370	0.022	0.018	0.000
7	0.030	0.008	0.005	0.003	0.000
8	0.000	0.001	-0.001	0.000	0.000
9	0.000	0.000	0.000	0.000	0.000

zation ($\delta_{\rm fit}$) and by those obtained from the solution of the Schrödinger equation containing the inversion potential (δ_I) are all quite good. The differences specified in columns 4 and 6 in the tables are very small except at low values of l, which is due to an l dependence of the K-model potential, which is averaged out by our l-independent inversion procedure. As expected, the differences are most pronounced for the $n-\alpha$ system at an incident neutron energy $E_n=50$ MeV. In all cases considered, the phase shifts for $l>7$ are almost identical.

The equivalent local potentials $V_I(E,R), V_L(E,R)$ as well as the one obtained from the Wigner transform via Eq. (4) [hereafter identified as $V^W(E,R)$] for the $n-\alpha$ system at $E_n=50$ MeV are shown in Fig. 1. They are displayed therein by the solid, dot-dashed, and dotted curves, respectively. In most of the interaction region the potentials have similar behavior, but they differ considerably at short distances. The variation of the inversion potential reflects the inherent l dependence of the phase shifts. In Fig. 2 the potentials for $n-\alpha$ scattering are shown at $E_n=100$ MeV and it is evident that the differences are less pronounced, a result not unexpected since the energy is relatively high for a light nuclear system.

The s-wave wave functions obtained from the solution of the Schrödinger equation with the inversion potential $V_I(E,R)$ and with the Wigner transform $V^W(E,R)$ are shown in Figs. 3 and 4 for $E_n=50$ MeV and $E_n=100$ MeV, respectively. The results are displayed by the solid and dashed

TABLE II. Same as Table I at $E_n=100$ MeV.

l	δ_K	$\delta_{\rm fit}$	$\delta_K-\delta_{\rm fit}$	δ_I	$\delta_K-\delta_I$
0	50.672	50.619	-0.052	49.416	-1.252
1	43.718	43.718	0.000	42.804	-0.854
2	30.234	30.187	-0.048	30.446	0.211
3	16.744	16.735	-0.010	17.218	0.474
3	7.794	7.759	-0.035	7.981	0.187
4	3.178	3.157	-0.021	3.223	0.045
5	1.160	1.145	-0.015	1.169	0.009
6	0.382	0.352	-0.031	0.384	0.002
7	0.115	0.081	-0.034	0.115	0.000
8	0.031	-0.005	-0.036	0.031	0.000
9	0.008	-0.030	-0.038	0.008	0.000

TABLE III. Same as Table I for the $n-{}^{40}$Ca system at $E_n=100$ MeV.

l	δ_K	$\delta_{\rm fit}$	$\delta_K-\delta_{\rm fit}$	δ_I	$\delta_K-\delta_I$
0	-59.273	-57.554	1.719	-57.815	-1.458
1	-58.467	-59.608	1.140	-60.107	-1.640
2	-63.472	-63.753	-0.281	-64.647	-1.175
3	-70.696	-70.269	0.427	-71.413	-0.717
3	-79.800	-79.282	0.517	-80.358	-0.558
4	89.333	89.251	-0.082	88.566	-0.767
5	76.651	75.718	-0.933	75.444	-1.206
6	60.841	60.666	-0.175	60.045	-0.196
7	44.925	44.923	-0.002	44.925	0.000
8	30.177	30.152	-0.024	30.177	0.000
9	18.354	18.242	-0.112	18.354	0.000
10	10.303	10.177	-0.125	10.303	0.000
11	5.452	5.376	-0.076	5.452	0.000
12	2.710	2.680	-0.031	2.710	0.000
13	1.236	1.278	-0.008	1.236	0.000
14	0.504	0.503	-0.001	0.504	0.000
15	0.181	0.182	0.001	0.181	0.000
16	0.057	0.057	0.000	0.057	0.000
17	0.016	0.010	0.000	0.010	0.000
18	0.001	0.001	0.000	0.004	0.000
19	0.000	0.000	0.000	0.001	0.000
20	0.000	0.000	0.000	0.000	0.000

TABLE IV. Same as Table I for the $n-{}^{40}$Ca system at $E_n=150$ MeV.

l	δ_K	$\delta_{\rm fit}$	$\delta_K-\delta_{\rm fit}$	δ_I	$\delta_K-\delta_I$
0	-77.488	-76.618	0.870	-77.089	0.0399
1	-77.937	-78.266	-0.330	-78.525	-0.589
2	-80.900	-81.047	-0.147	-81.397	-0.497
3	-85.252	-85.246	0.006	-85.638	-0.386
3	89.063	89.097	0.036	88.756	-0.306
	82.175	82.096	-0.079	81.884	-0.291
5	74.096	73.810	-0.286	73.757	-0.340
6	64.622	64.501	-0.120	64.564	-0.057
7	54.469	54.374	-0.095	54.469	0.000
8	43.946	43.873	-0.073	43.946	0.000
9	33.595	33.556	-0.039	33.595	0.000
10	24.207	24.177	-0.030	24.207	0.000
11	16.483	16.425	-0.058	16.483	0.000
12	10.618	10.546	-0.072	10.618	0.000
13	6.508	6.442	-0.066	6.508	0.000
14	3.837	3.768	-0.068	3.837	0.000
15	2.170	2.095	-0.075	2.170	0.000
16	1.152	1.083	-0.050	1.152	0.000
17	0.559	0.509	-0.050	0.559	0.000
18	0.242	0.214	-0.029	0.242	0.000
19	0.093	0.080	-0.014	0.093	0.000
20	0.032	0.026	-0.006	0.032	0.000

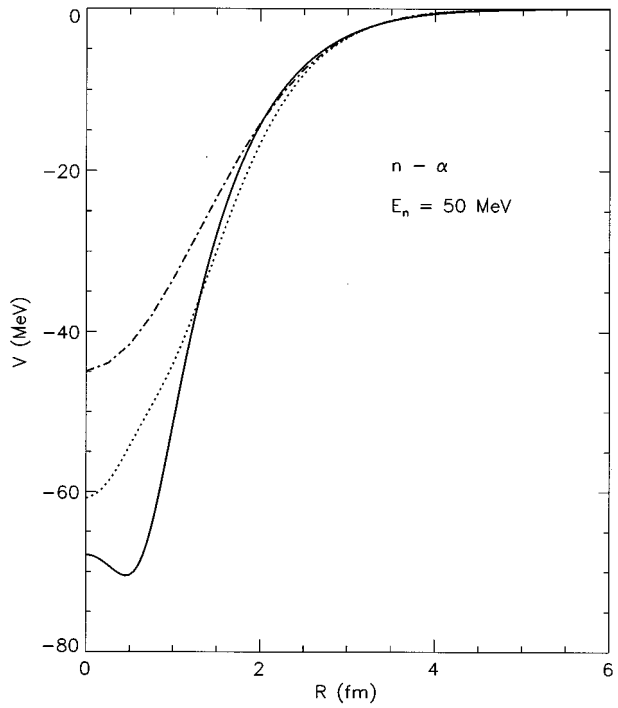

FIG. 1. Equivalent local potentials obtained by inversion $V_I(E,R)$ (solid curve), by the Horiuchi method $V_L(E,R)$ (dot-dashed curve), and via the Wigner transform $V^W(E,R)$ (dotted curve), for the $n-\alpha$ system at an incident neutron energy $E_n=50$ MeV.

curves, respectively. It is seen that the large differences in the potentials at short distances are not manifested strongly in the characteristics of the wave functions. At $E_n=100$ MeV the two wave functions beyond $R>1.5$ fm are in excellent agreement. For the $n-^{40}$Ca system, the behavior of the potentials and the wave functions is quantitatively and qualitatively better than for the $n-\alpha$ results. The potentials are shown in Figs. 5 and 6 and the corresponding $l=0$ wave functions in Figs. 7 and 8 for $E_n=100$ MeV and $E_n=150$ MeV, respectively. For $E_n=150$ MeV, the potentials and the wave functions are identical for all practical purposes.

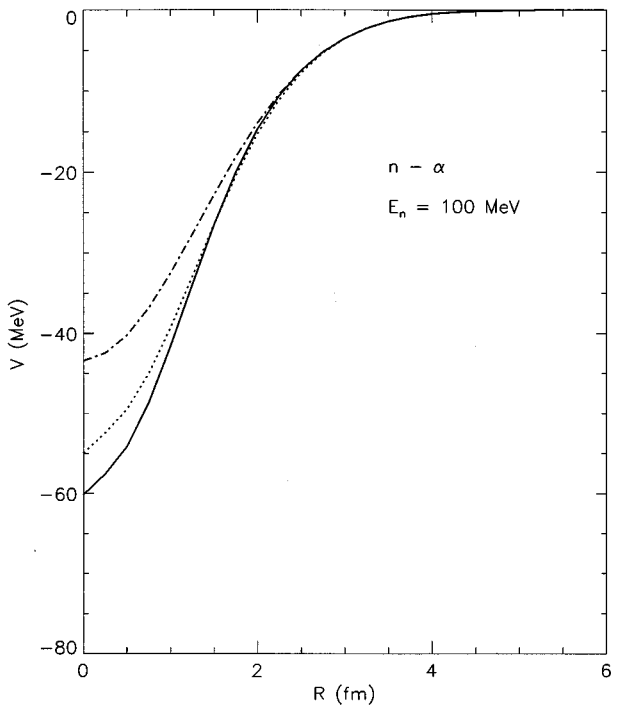

FIG. 2. Same as Fig. 1, but at $E_n=100$ MeV.

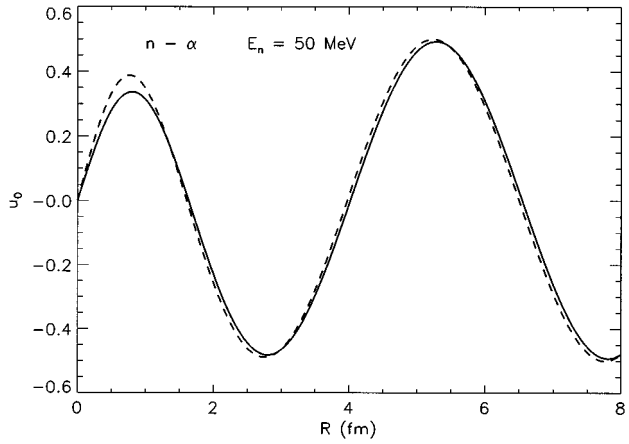

FIG. 3. Comparison of the s-wave wave functions obtained from the solution of the Schrödinger equation with the Wigner transform $V^W(E,R)$ (solid curve) and with the inversion potential $V_I(E,R)$ (dashed curve) for the $n-\alpha$ system at an incident neutron energy $E_n=50$ MeV.

The better quality of the results for both systems at higher energies is not unexpected and is due to the fact that the l-independent inversion scheme and the WKB approximation, on which our method is based, are better justified. With respect to the different systems, the overall better quality of the results for the $n-^{40}$Ca system can be attributed to the fact that, in that case, the l dependence of the starting K model is weak and the quality of the WKB approximation is better. We also note that the validity of the K model improves as the mass of the target nucleus increases.

IV. CONCLUSIONS

The energy-dependent, quantal inversion scheme of Lipperheide and Fiedeldey [13], which utilizes phase shifts δ_l,

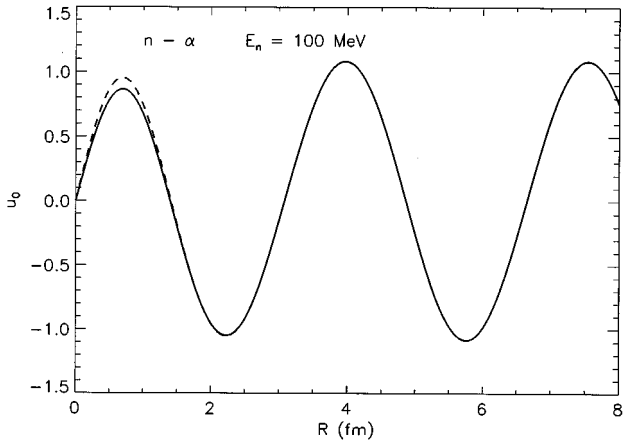

FIG. 4. Same as Fig. 3, but at $E_n=100$ MeV.

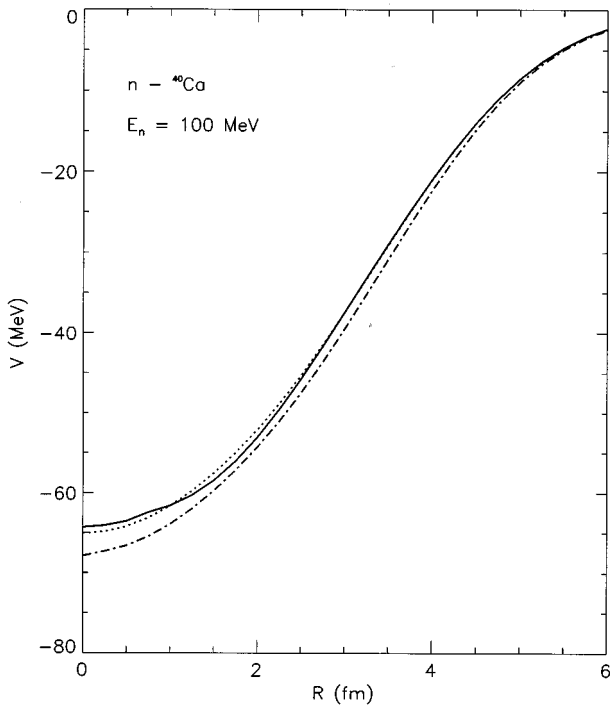

FIG. 5. Equivalent local potentials obtained by inversion $V_I(E,R)$ (solid curve), by the Horiuchi method $V_L(E,R)$ (dot-dashed curve), and via the Wigner transform $V^W(E,R)$ (dotted curve), for the $n+^{40}$Ca system at an incident neutron energy $E_n=100$ MeV.

$l=1,2,\ldots,N$, has given local potentials in good agreement with those found within the WKB approximation, as the Wigner transforms of a class of nonlocal interactions. The interactions from the so-called K model, a simplified version

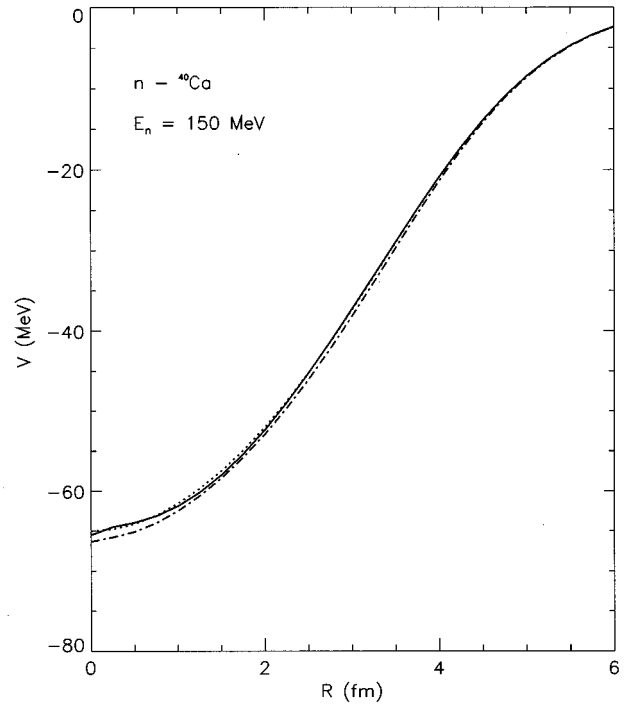

FIG. 6. Same as Fig. 5, but at $E_n=150$ MeV.

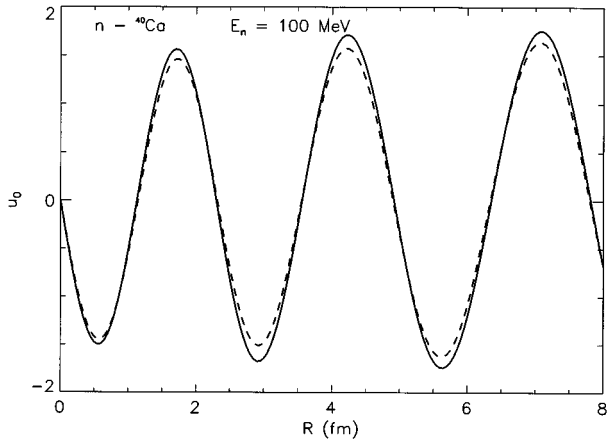

FIG. 7. Comparison of the s-wave wave functions obtained from the solution of the Schrödinger equation with the Wigner transform $V^W(E,R)$ (solid curve) and with the inversion potential $V_I(E,R)$ (dashed curve) for the $n+^{40}$Ca system at an incident neutron energy $E_n=100$ MeV.

of the microscopically derived RGM nonlocal potentials, were used as the test cases. These interactions are a special class of nonlocal interactions as they are energy independent and have Wigner transforms that are l independent. We have chosen to use these interactions because of their simplicity despite the obvious drawback that spin-orbit effects are averaged out and are not taken into account explicitly.

With these limitations in mind, two systems have been studied. With these systems we have demonstrated that the method works well within the limits in which the WKB approximation and the K model are valid. The results show a good agreement of the equivalent local potentials obtained by inversion and via the Wigner transform. The agreement of the $l=0$ wave functions found using the two interactions also is good.

Of course the nonlocality has not been reconstructed, but this can be done by an inverse Fourier transformation, which requires implementation of the scheme at a large number of energies, a task that is beyond the scope of this work. In a case such as $n-^{40}$Ca, this could be done directly from the experimental phase shifts if they are available at a suffi-

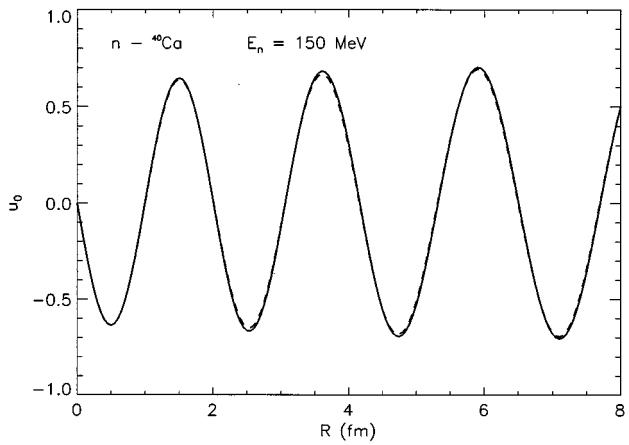

FIG. 8. Same as Fig. 7, but at $E_n=150$ MeV.

ciently large number of energies. The results could then be compared to those of the K model.

ACKNOWLEDGMENTS

This work was initiated by stimulating discussions with the late Professor H. Fiedeldey. One of us (G. P.) gratefully acknowledges the financial support from Foundation for Research Development and the University of South Africa.

APPENDIX: EVALUATION OF THE PARAMETERS α_n AND β_n

In order to evaluate the complex parameters α_n and β_n we rewrite the S function as

$$S_\lambda = \frac{1+\Sigma_{m=1}^{N} B_m z^m}{1+\Sigma_{m=1}^{N} A_m z^m}, \tag{A1}$$

where $\lambda = l+1/2$, $l=0,1,\ldots,2N$; A_m and B_m are, in general, complex coefficients; and $z=1/\lambda^2$. The roots of the polynomials

$$1+\sum_{m=1}^{N} B_m z^m = 0 \tag{A2}$$

and

$$1+\sum_{m=1}^{N} A_m z^m = 0 \tag{A3}$$

provide us with the values of α_m^{-2} and β_n^{-2}, respectively. The coefficients A_m and B_n can be determined if we rewrite Eq. (A1) in the form

$$S_\lambda \sum_{m=1}^{N} A_m z^m - \sum_{m=1}^{N} B_m z^m = 1 - S_\lambda \tag{A4}$$

or in a matrix notation

$$\sum_{k=1}^{2N} M_{lk} x_k = y_k, \tag{A5}$$

where

$$x_k = \begin{cases} A_m, & k=m \quad m=1,2,\ldots,N \\ B_m, & k=N+m, \quad m=1,2,\ldots,N \end{cases} \tag{A6}$$

and

$$M_{lk} = \begin{cases} S_l z^k, & k=1,2,\ldots,N \\ -z^{k-N}, & k=N+1,N+2,\ldots,2N. \end{cases} \tag{A7}$$

Furthermore,

$$y_k = 1 - S_l, \quad l=0,1,\ldots,2N. \tag{A8}$$

Thus the task of evaluating the α_m and β_m is reduced to the solution of the system (A5) to obtain the B_n and A_m and then to locate the roots of the polynomials (A2) and (A3).

[1] H. Fiedeldey, Nucl. Phys. **A135**, 333 (1969); H. Fiedeldey, S. A. Sofianos, L.J. Allen, and R. Lipperheide, Phys. Rev. A **32**, 3095 (1985); **33**, 1581 (1986).

[2] H. Feshbach, Ann. Phys. (N.Y) **5**, 357 (1958); **19**, 287 (1962); G. R. Satchler and W. G. Love, Phys. Rep. **C 55**, 183 (1979); M. Tretz, A. Faessler, and D. H. Dickhoff, Nucl. Phys. **A443**, 499 (1985); K. Wildermuth and Y. C. Tang, *A Unified Theory of the Nucleus* (Vieweg, Braunschweig, 1977).

[3] T. Kaneko, M. LeMere, and Y. C. Tang, Phys. Rev. C **44**, 1558 (1991).

[4] T. Kaneko, M. LeMere, and Y. C. Tang, Phys. Rev. C **46**, 298 (1992).

[5] G. Pantis, S. A. Sofianos, H. Fiedeldey, R. Lipperheide, and P. F. Hodgson, Nucl. Phys. **A559**, 266 (1993); G. Pantis, H. Fiedeldey, and S. A. Sofianos, *ibid.* **565**, 628 (1993).

[6] M. Lassaut and N. Vinh Mau, Phys. Lett. **70B**, 321 (1972); Nucl. Phys. **A349**, 372 (1980).

[7] H. Horiuchi, Prog. Theor. Phys. **46**, 184 (1980); **59**, 516 (1983); K. Aoki and H. Horiuchi, *ibid.* **68**, 1652 (1982).

[8] S. Karataglidis, P. J. Dortmans, K. Amos, and R. de Swiniarski, Phys. Rev. C **52**, 861 (1995); **53**, 838 (1966).

[9] G. Pantis and J. M. Pearson, Phys. Rev. C **36**, 1408 (1987).

[10] H. G. Bohlen, E. Stiliaris, B. Gebauer, W. von Oertzen, M. Wilpert, Th. Wilpert, A. Ostrowski, Dao T. Khoa, A. S. Demyanowa, and A. A. Ogloblin, Z. Phys. A **346**, 189 (1993).

[11] G. Pantis, R. Linden, N. Ohtsuka, and A. Faessler, Nucl. Phys. **A449**, 209 (1989).

[12] S. A. Sofianos, H. Fiedeldey, R. Lipperheide, G. Pantis, and P. E. Hodgson, Nucl. Phys. **A540**, 199 (1992).

[13] R. Lipperheide and H. Fiedeldey, Z. Phys. A **286**, 45 (1978); **301**, 81 (1981).

[14] K. Naidoo, H. Fiedeldey, S. A. Sofianos, and R. Lipperheide, Nucl. Phys. **A419**, 13 (1984).